Mol. Cells *29*, 387-395, April 30, 2010
DOI/10.1007/s10059-010-0039-6

Molecules and Cells

IP_3-Induced Cytosolic and Nuclear Ca^{2+} Signals in HL-1 Atrial Myocytes: Possible Role of IP_3 Receptor Subtypes

Joon-Chul Kim, Min-Jeong Son, Krishna P. Subedi, Do Han Kim[1], and Sun-Hee Woo*

HL-1 cells are the adult cardiac cell lines available that continuously divide while maintaining an atrial phenotype. Here we examined the expression and localization of inositol 1,4,5-trisphosphate receptor (IP_3R) subtypes, and investigated how pattern of IP_3-induced subcellular local Ca^{2+} signaling is encoded by multiple IP_3R subtypes in HL-1 cells. The type 1 IP_3R (IP_3R1) was expressed in the perinucleus with a diffuse pattern and the type 2 IP_3R (IP_3R2) was expressed in the cytosol with a punctate distribution. Extracellular ATP (1 mM) elicited transient intracellular Ca^{2+} releases accompanied by a Ca^{2+} oscillation, which was eliminated by the blocker of IP_3Rs, 2-APB, and attenuated by ryanodine. Direct introduction of IP_3 into the permeabilized cells induced Ca^{2+} transients with Ca^{2+} oscillations at $\geq$ 20 μM of IP_3, which was removed by the inhibition of IP_3Rs using 2-APB and heparin. IP_3-induced local Ca^{2+} transients contained two distinct time courses: a rapid oscillation and a monophasic Ca^{2+} transient. The magnitude of Ca^{2+} oscillation was significantly larger in the cytosol than in the nucleus, while the monophasic Ca^{2+} transient was more pronounced in the nucleus. These results provide evidence for the molecular and functional expression of IP_3R1 and IP_3R2 in HL-1 cells, and suggest that such distinct local Ca^{2+} signaling may be correlated with the punctate distribution of IP_3R2s in the cytosol and the diffuse localization of IP_3R1 in the peri-nucleus.

INTRODUCTION

Inositol 1,4,5-trisphosphate receptors (IP_3Rs) are ubiquitous intracellular Ca^{2+} release channels that are regulated by Ca^{2+} and IP_3, and mediate the rise in intracellular Ca^{2+} in response to the receptor-activated production of IP_3 (Berridge, 2005). Phosphatidylinositol 4,5-bisphosphate turnover, coupled to endothelin, adrenergic, and purinergic receptors, has been shown to increase IP_3 levels in cardiac muscle (Woodcock and Matkovich, 2005). Although the ryanodine receptors (RyRs) are the main pathway of Ca^{2+} release from the sarcoplasmic reticulum (SR) during excitation-contraction coupling in cardiac muscle, IP_3Rs, expressed in cardiac myocytes at lower levels, are also thought to play a role in regulating Ca^{2+} signaling under hormonal stimulation (Lipp et al., 2000; Moschella and Marks, 1993; Perez et al., 1997).

The compositions and subcellular localizations of IP_3R subtypes are somewhat different among the cell types, and are thought to be important in determining the spatio-temporal pattern of IP_3-dependent local Ca^{2+} signals (i.e. Ca^{2+} oscillation) in a specific cell type (Hattori et al., 2004; Miyakawa et al., 1999). This, in turn, underlies region- and subtype-specific functions, such as apoptosis (Mendes et al., 2005) and gene transcription (Wu et al., 2006). However, the spatio-temporal pattern of IP_3/IP_3R-mediated local Ca^{2+} signaling and the pathophysiological roles of the IP_3R-dependent Ca^{2+} signaling in cardiac myocytes are not fully understood.

HL-1 cells were derived from the adult atria of a transgenic mouse expressing the SV40 large T antigen under the control of the atrial natriuretic factor promoter (Claycomb et al., 1998). Because HL-1 cells are the only cells available that continuously divide and retain an adult cardiac phenotype in culture (Claycomb et al., 1998), they may serve as suitable adult cell culture systems to study cardiac muscle structure and function *in vitro* using genetic engineering techniques (White et al., 2004). Cultured embryonic and neonatal cardiac myocytes have also been widely used to study cardiac molecular physiology *in vitro*. However, they lack many of the characteristics of adult cardiac cells and they are overgrown by non-myocytes after a few days in culture. HL-1 cells generate autorhythmic Ca^{2+} transients (Sartiani et al., 2002) and express key ion channels underlying action potential and Ca^{2+}-induced Ca^{2+} release (White et al., 2004). α_1-adrenergic receptors and putative endothelin receptors that are coupled to inositol 1,4,5-trisphosphate (IP_3) production, have been characterized in these cells (Kitta et al., 2001; McWhinney et al., 2000). However, little is known about the presence of IP_3Rs in HL-1 cells.

The purpose of the present study was to search for the presence and localization of IP_3R subtypes in HL-1 cells, and to examine the spatio-temporal characteristics of local Ca^{2+} sig-

College of Pharmacy, IDRD, Chungnam National University, Daejeon 305-764, Korea, [1]Department of Life Science, Gwangju Institute of Science and Technology, Gwangju 500-712, Korea
*Correspondence: shwoo@cnu.ac.kr

Received October 28, 2009; revised November 30, 2009; accepted December 7, 2009; published online March 4, 2010

Keywords: Ca^{2+} oscillation, confocal imaging, HL-1 cell, local Ca^{2+} signal, localization, IP_3R subtypes

nals mediated by the IP_3Rs. Our data suggest that HL-1 cells express type 1 and type 2 IP_3Rs, similar to adult atrial myocytes, and that two subtypes in the HL-1 cells may mediate distinct local Ca^{2+} signals in different subcellular locations.

MATERIALS AND METHODS

Culture of HL-1 cells

HL-1 cardiomyocytes were obtained from Dr. W.C. Claycomb (Louisiana State University Health Science Center, USA), who first established and characterized the cell line (Claycomb et al., 1998). HL-1 cells were handled as previously described (Claycomb et al., 1998). HL-1 cells were grown onto a matrix of gelatin (0.02%, Difco) plus fibronectin (12.5 mg/ml, Sigma), into a medium consisting of Claycomb medium (JRH Biosciences, USA), 10% fetal bovine serum (JRH Biosciences), 4 mM L-glutamine (Life Technologies), 10 mM norepinephrine (Sigma), and 10 mM penicillin-streptomycin (Life Technologies). The cells were incubated at 37°C in 95% O_2-5% CO_2 at a relative humidity of 95%. The cells were plated 2 days before the experiment.

Isolation of cardiac myocytes

Rat ventricular myocytes were enzymatically isolated from male Sprague Dawley rats (200-300 g) as described previously (Lee et al., 2008). Briefly, rats were deeply anesthetized with sodium pentobarbital (150 mg/kg, i.p.), the chest cavity was opened, and the hearts were excised. This surgical procedure was carried out in accordance with the university's ethical guidelines. The excised hearts were retrogradely perfused at 7 ml/min through the aorta, first for 3 min with a Ca^{2+}-free Tyrode solution composed of (in mM): 137 NaCl, 5.4 KCl, 10 HEPES, 1 $MgCl_2$, 10 glucose, and pH 7.3, at 36.5°C; and then with a Ca^{2+}-free Tyrode solution containing collagenase (1.4 mg/ml, Type 1, Roche) and protease (0.14 mg/ml, Type XIV, sigma) for 12 min; and finally with Tyrode solution containing 0.2 mM $CaCl_2$ for 8 min. The ventricles and atria of the digested heart were then cut into several sections and subjected to gentle agitation to dissociate the cells. The freshly dissociated cells were stored at room temperature in Tyrode solution containing 0.2 mM $CaCl_2$.

Reverse transcription and polymerase chain reaction (RT-PCR)

Total RNA was prepared from cells using the TRIzol reagent (Invitrogen Co., USA). cDNA was synthesized from total RNA using PrimeScript reverse transcriptase (Takara Bio Inc., Japan), following the manufacturer's instructions, with 100 ng oligo-dT as a primer (19 bp; Bioneer Co., Korea). The RNA samples were denatured at 65°C for 5 min and RT was performed at 42°C for 2 h. PCR for IP_3Rs was performed by using primers that were designed based on the published sequences of mouse IP_3Rs mRNA (GenBank accession No.: IP_3R1, NM_010585; IP_3R2, AB182288; and IP_3R3, NM_080553). The primers used were 5′-GCTTCTACAATCCTACGACTG-3′ and 5′-CCTCAGGTCAGCAAAGGTGTC-3′ for IP_3R1, 5′-CCTGGCTGTGTTCATCAACCT-3′ and 5′-GGGCTCATCTTTCGAGGGTCG-3′ for IP_3R2, and 5′-GGATCCTCATCTGCTTCTCCA-3′ and 5′-CGATGATCACCCCAAAGATGA-3′ for IP_3R3. The general PCR conditions were 2 μl of the reverse transcription products, each corresponding to 200 ng of initial total RNA, 0.2 mM of dNTP, PrimeSTAR buffer, and PrimeSTAR HS-DNA polymerase (Takara Bio Inc.), and each primer in a total volume of 25 μl. The cDNA samples were initially denatured at 98°C for 3 min followed by 25 cycles of 98°C for 10 s, 55°C for 5 s, and 72°C for 1 min, and a 10-min final extension. As a positive control, β-actin was amplified using the same protocol with primers 5′-GGAATCCTGTGGCATCCATG-3′ and 5′-CGTACTCCTGCTTGCTGATCC-3′, designed based on the mouse cytoplasmic β-actin mRNA (AC: M12481). The amplified products (10 μl each) were separated by electrophoresis on 1.5% agarose gels and stained with ethidium bromide.

Sodium dodecyl sulfate-polyacrylamide gel electrophoresis and Western blotting

A total of 50 μg of total protein extract from isolated cardiac cells or from HL-1 cells were subjected to Western blot analysis as described previously (Hong, 2002). The antibodies against IP_3R1 (rabbit polyclonal IgG, 1:1000; Chemicon International Inc., USA), IP_3R2 (goat polyclonal IgG, 1:200; Santa Cruz Biotechnology, Inc., USA), IP_3R3 (monoclonal IgG, 1:1000; Transduction Laboratories, USA), and α-actinin (polyclonal IgG, 1:1000; Santa Cruz Biotechnology Inc.) were purchased.

Immunocytochemistry

HL-1 cells were fixed in 4% paraformaldehyde (in phosphate-buffered saline solution, PBS) for 10 min and permeabilized with 0.1% Triton X-100 for 10 min. After the cells were incubated in PBS containing 1% BSA (Sigma-Aldrich Inc., USA) for 1 h to block nonspecific labeling, they were incubated with the antibodies for IP_3R1 (rabbit polyclonal IgG, 0.45 μg/ml; Chemicon International Inc.), IP_3R2 (goat polyclonal IgG, 0.3 μg/ml; Santa Cruz Biotechnology Inc.), and/or LAP2 (mouse polyclonal IgG, 0.25 μg/ml; BD Biosciences Co., USA) overnight at 4°C. The primary antibodies for IP_3R1 were detected using the Alexa Fluor 488 conjugated polyclonal antibody specific to rabbit (1:1000 dilution; Molecular Probes; 1 h, RT), and those for IP_3R2 and LAP2 were detected using the Alexa Fluor 568 conjugated polyclonal antibody specific to goat and to mouse, respectively (1:1000 dilution; Molecular Probes; 1 h, RT). After the cover slips were mounted with Mowiol antifadent medium (Sigma), fluorescence images of 512 × 512 pixels were acquired with a confocal microscope (Zeiss, LMS 510, Germany).

Permeabilization of HL-1 cells

HL-1 cells were permeabilized with saponin using a modified procedure from Lukyanenko and Györke (1999). First, the cells were suspended in a solution containing (mM) potassium aspartate 100, KCl 20, EGTA 0.5, $MgCl_2$ 0.75, and HEPES 10 (pH 7.2, titrated with KOH). The cell membrane was permeabilized by adding 0.01% (w/v) saponin for 1 min 40 s. The bathing solution was then exchanged for a saponin-free internal solution composed of (mM) potassium aspartate 100, KCl 15, KH_2PO_4 5, MgATP 5, $CaCl_2$ 0.0002, $MgCl_2$ 0.75, phosphocreatine 10, creatine phosphokinase 5 U/ml, dextran (Mr: 40,000) 8%, HEPES 10 and fluo-3 pentapotassium salt 0.04 (pH 7.2, titrated with KOH). After 4 min, the bathing solution was exchanged for a dye-free internal solution.

Confocal Ca^{2+} imaging

Ca^{2+} fluorescence was imaged at 2.38 Hz using a laser scanning confocal microscopy system (C1 Eclipse, Nikon, Japan) fitted with a × 60 oil-immersion objective lens (Plan Apo, numerical aperture 1.4, Nikon), as previously described (Lee et al., 2008). In some experiments, HL-1 cells were loaded with fluo-4 AM (3 μM) for 30 min (Fig. 4). The dyes were excited at 488 nm using an Ar ion laser and fluorescence emissions at wavelengths > 510 nm were detected. The measurements of Ca^{2+} fluorescence were followed by examining the nucleus in the same cell with the nucleic acid dye, syto-11 (2.5 μM, 30 s; Molecular Probes). The excitation and emission of syto-11 were

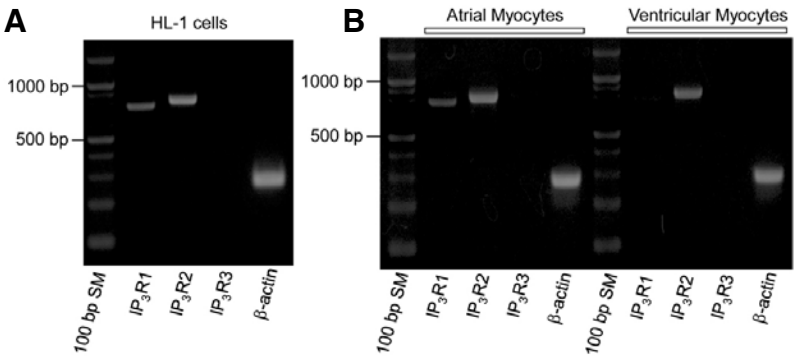

Fig. 1. RT-PCR analysis of IP_3R gene expression in HL-1 cells, and in adult rat atrial and ventricular myocytes. Truncated regions of IP_3R1, 2, 3 and β-actin were amplified with specific primers (see "Materials and Methods") using 10 ng of total RNA from HL-1 cells (A), and atrial and ventricular myocytes (B). β-actin was used as a housekeeping gene. The left lane for each cell type represent low DNA mass ladders (bp = base pairs, GIBCO-BRL; SM = size marker). The predicted sizes of IP_3R1, IP_3R2, IP_3R3, and β-actin were 737 bp, 831 bp, 822 bp, and 281 bp, respectively.

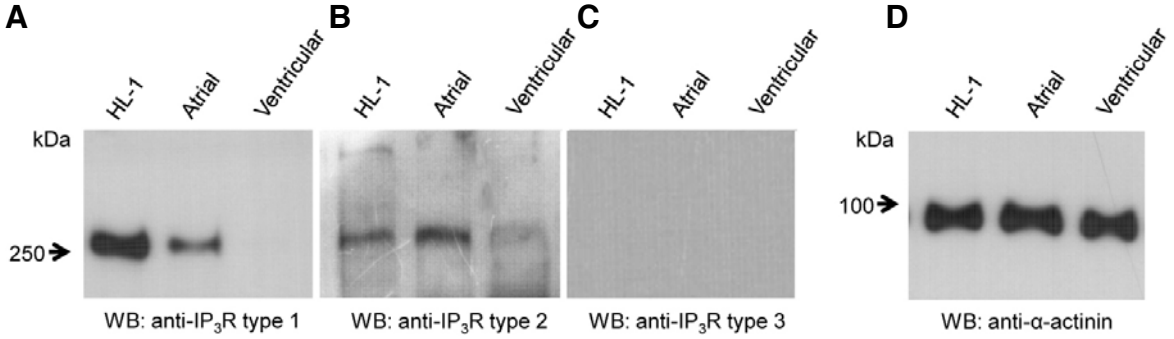

Fig. 2. Expression of IP_3 receptors in HL-1 cells and isolated adult rat cardiomyocytes. Representative immunoblots showing expression level of IP_3R1 (A), IP_3R2 (B) and IP_3R3 (C), in HL-1 cells, adult rat atrial myocytes ("Atrial") and ventricular myocytes ("Ventricular"). As a loading control α-actinin was used (D). Details were described under "Materials and Methods."

the same as those of fluo-4. Since the emission of syto-11 was much brighter than that of fluo-4, only the syto-11 fluorescence could be visualized by decreasing the PMT power. The average resting fluorescence intensity (F_0) was calculated from several frames measured before the interventions. Tracings of Ca^{2+} signals from the regions-of-interest (ROI) were shown as the average fluorescence of each area normalized relative to the F_0 (F/F_0) (Kim et al., 2008).

IP_3 (*D-myo*-inositol 1,4,5-trisphosphate trisodium salt; Calbiochem, USA) was dissolved in the saponin- and dye-free internal solution (see *above*) containing tetracaine (1 mM; Sigma), and applied to the cell by using rapid solution exchange system. 2-aminoethoxydiphenyl borate (2-APB) and heparin were purchased from the Sigma Corporation and the Choongwae Pharma Corporation (Korea), respectively. The ATP (Na^+ salt)-containing solution also included 0.5 mM EGTA to remove contaminated Ca^{2+} in the zero Ca^{2+} Tyrode solution.

Statistics

Numerical results are given as mean ± standard error of mean (S.E.M.) (n = number of cells). Statistical comparisons were carried out using Student's *t*-tests. Differences were considered to be statistically significant to a level of $P < 0.05$.

RESULTS

Molecular identification of IP_3Rs in HL-1 cells

We examined the molecular expression of the IP_3R isoforms in HL-1 compared with that of atrial and ventricular cells using RT-PCR. Products of the expected sizes were obtained for the IP_3R1 (lane 2; 737 bp) and IP_3R2 (lane 3; 831 bp) in HL-1 cells (Fig. 1A). RT-PCR analysis failed to identify the IP_3R3 in these cells. The β-actin mRNA band (lane 5) was shown as a positive control. The same experiments using isolated adult rat atrial and ventricular myocytes revealed that both IP_3R1 and IP_3R2 were expressed in rat atrial myocytes (lanes 2 and 3, Fig. 1B), and that only IP_3R2 was expressed in rat ventricular myocytes (lane 8, Fig. 1B).

We next examined the expression of IP_3R proteins in HL-1 cells compared with atrial and ventricular myocytes by using specific antibodies directed against IP_3R1, IP_3R2, and IP_3R3. The expression of both IP_3R1 and IP_3R2 was detected in rat atrial myocytes and HL-1 cells, whereas only IP_3R2 was detected in ventricular myocytes (Figs. 2A and 2B). The expression of IP_3R3 was not detected in any of the three types of cells under the standard conditions used (Fig. 2C). The density of IP_3R1 was significantly higher in HL-1 cells compared with that in isolated atrial myocytes (Fig. 2A), whereas the expression of IP_3R2 was slightly higher in isolated atrial cells than in HL-1 cells (Fig. 2B). The protein level of IP_3R2 was the lowest in ventricular myocytes (Fig. 2B).

Immunolocalization of IP_3R1 and IP_3R2 in HL-1 cells

Since we found the expression of IP_3R1 and IP_3R2 in HL-1 cells, we next checked the subcellular distribution of the IP_3R subtypes in HL-1 cells using an immunostaining technique with specific antibodies against IP_3R1 and IP_3R2. The IP_3R1 was mainly distributed around the nucleus (Fig. 3A, *green*) and co-localized with lamina-associated polypeptide 2 (LAP2), an integral protein in the inner membrane of the nuclear envelope with the majority of its structure exposed to the nucleoplasm (Furukawa et al., 1995) (see *yellow dots* in the image labeled as "*IP_3R1 + LAP2*" in Fig. 3A). LAP2 is known to contribute to the attachment of the nuclear lamina to the inner nuclear mem-

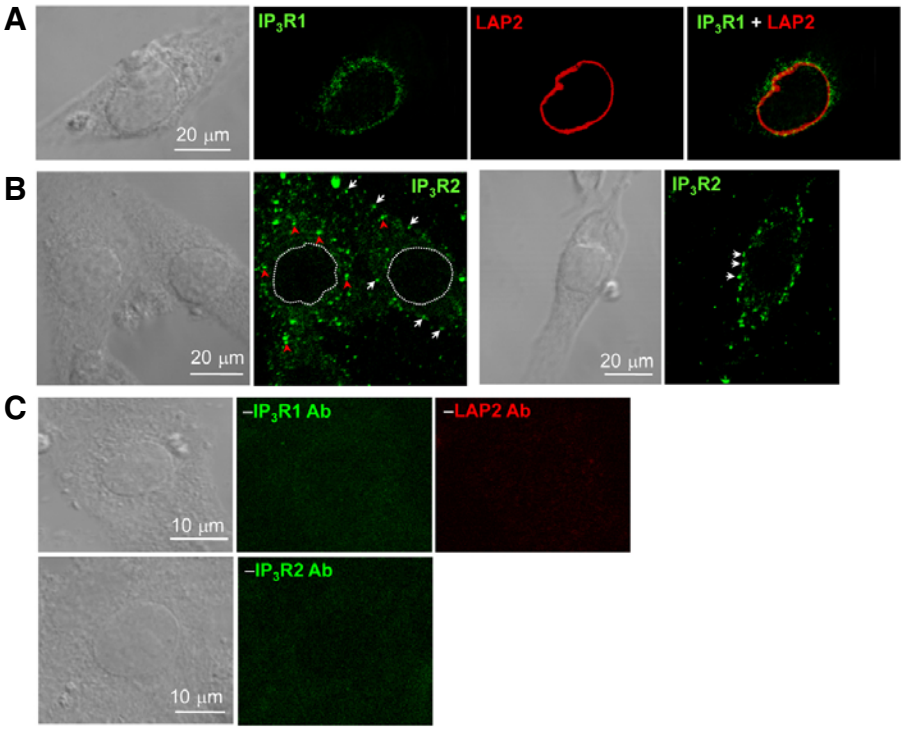

Fig. 3. Subcellular localizations of IP_3R1 and IP_3R2 in HL-1 cells. (A) IP_3R1 signal was shown as green color in the second image. All images were recorded by confocal microscope (see "Materials and Methods"). LAP2, an inner membrane integral protein in the nuclear envelope, was stained as red color. Superimposed image of IP_3R1- and LAP2-signals shows co-localization of those proteins at specific spots (*yellow*). (B) Immunostained images of two representative types of HL-1 cells for IP_3R2 (*green*). Cells at ~90%- and ~60%-confluence were displayed in the left and right images, respectively. (C) Images of HL-1 cells treated with the same immunostainig protocol but with no primary antibodies.

brane (Furukawa et al., 1995). The IP_3R2, in contrast, was localized to the cytoplasm as a punctate form (Fig. 3B). In cells with a confluence of $\leq$ 60%, the IP_3R2 was largely distributed in the peripheral regions (white arrows in right images, Fig. 3B), whereas in cells with high confluence (> ~80%), it was localized to specific sites in both the interior (red arrows in Fig. 3B) and periphery of the cytoplasm (left images, Fig. 3B). We used the cells with > 80% confluence for Ca^{2+} imaging experiments.

ATP-induced Ca^{2+} oscillation via IP_3Rs in HL-1 cells

To investigate whether the IP_3Rs regulate Ca^{2+} signal in HL-1 cells, a high concentration (1 mM) of extracellular ATP, known to generate IP_3 via PLCγ (Pucéat and Vassort, 1996) and induce the release of intracellular Ca^{2+} in cardiac myocytes (Danziger et al., 1988; Jaconi et al., 2002), was used to record IP_3-induced Ca^{2+} releases. The autorhythmic Ca^{2+} transients in HL-1 cells were suppressed by superfusing a zero Ca^{2+} Tyrode solution. In the absence of external Ca^{2+}, 1 mM ATP induced Ca^{2+} oscillations (Fig. 4Aa). The pattern of ATP-induced Ca^{2+} oscillation varied somewhat from cell to cell (Left traces in "*a-c*" of Fig. 4A). Repeated application of 1 mM ATP in the same cells continued to elicit Ca^{2+} oscillation (see "*ATP (1 mM, 2nd)*" in Fig. 4Aa), although the magnitude ($\Delta F/F_0$) of the Ca^{2+} change was reduced by ~30% during the second applications (1st, 4.4 $\pm$ 0.54; 2nd, 2.9 $\pm$ 0.45; n = 24, P < 0.05, 1st *vs* 2nd trials; Fig. 4C). Such a reduction of Ca^{2+} change on the second application of ATP might be caused by the agonist-induced desensitization of the ATP receptor (Flores et al., 2005; Lin and Chuang, 1993) and/or a possible decrease in SR Ca^{2+} content brought about by the long-term exposure to zero Ca^{2+} solution. Since there was no Ca^{2+} in the bath solutions, the Ca^{2+} increase, induced by ATP, might be caused by Ca^{2+} releases from the internal store.

To test whether the RyR was involved in the Ca^{2+} increases during the ATP exposure, the effects of ATP were examined in the presence of ryanodine (20 μM), the RyR blocker. After the ATP response was recorded under the control conditions, the Ca^{2+} changes, induced by the 2nd exposure to ATP, were monitored in the same cells pre-treated with ryanodine for 5 min (Fig. 4Ab). ATP continued to generate Ca^{2+} oscillations in the ryanodine-pretreated HL-1 cells (Fig. 4Ab), but their magnitudes ($\Delta F/F_0$: 1.0 $\pm$ 0.2, n = 18) were significantly smaller than those (2.9 $\pm$ 0.45, n = 24) measured during the 2nd applications of ATP in the absence of ryanodine (compare "*ATP (2nd)*" and "*rya, ATP (2nd)*" in Fig. 4C; P < 0.001). Next, we tested if IP_3Rs are responsible for the ATP-mediated Ca^{2+} mobilization using the blocker of IP_3Rs, 2-APB, which has been used successfully to inhibit IP_3R-dependent Ca^{2+} release in cardiac cells at the concentration used (Bootman et al., 2002; Mackenzie et al., 2002; Zima and Blatter, 2004). The cells, which had shown the ATP response, failed to produce significant Ca^{2+} changes after they were pre-exposed to 5 μM 2-APB (Fig. 4Ac; n = 11, P < 0.001, "*ATP (2nd)*" *vs.* "*2-APB, ATP (2nd)*" in Fig. 4C). We also confirmed that the pre-exposure to 20 μM of ryanodine for 5 min was enough to block RyR-mediated Ca^{2+} releases through the use of 10 mM caffeine, the activator of RyR (Fig. 4B). These results suggest that ATP-induced Ca^{2+} oscillation is initiated by the activation of the IP_3Rs, and provide an evidence for a function of IP_3Rs in intact HL-1 cells. The results also indicate that the Ca^{2+}-induced Ca^{2+} release through the RyRs may contribute to the rise of Ca^{2+} in the presence of ATP.

IP_3-induced local Ca^{2+} signal in permeabilized HL-1 cells

In the next series of experiments, we investigated the spatiotemporal properties of IP_3-induced *local* Ca^{2+} signals in the cytosol and nucleus of HL-1 cells. Different concentrations of IP_3 were directly introduced into the HL-1 myocytes using the membrane permeabilization method. The position of the nucleus was localized in each cell tested by staining the cells with the nucleic acid dye syto-11 (see "Materials and Methods") immediately after the Ca^{2+} imaging. To exclude Ca^{2+} release through the RyRs, cells were pre-incubated with 1 mM tetra-

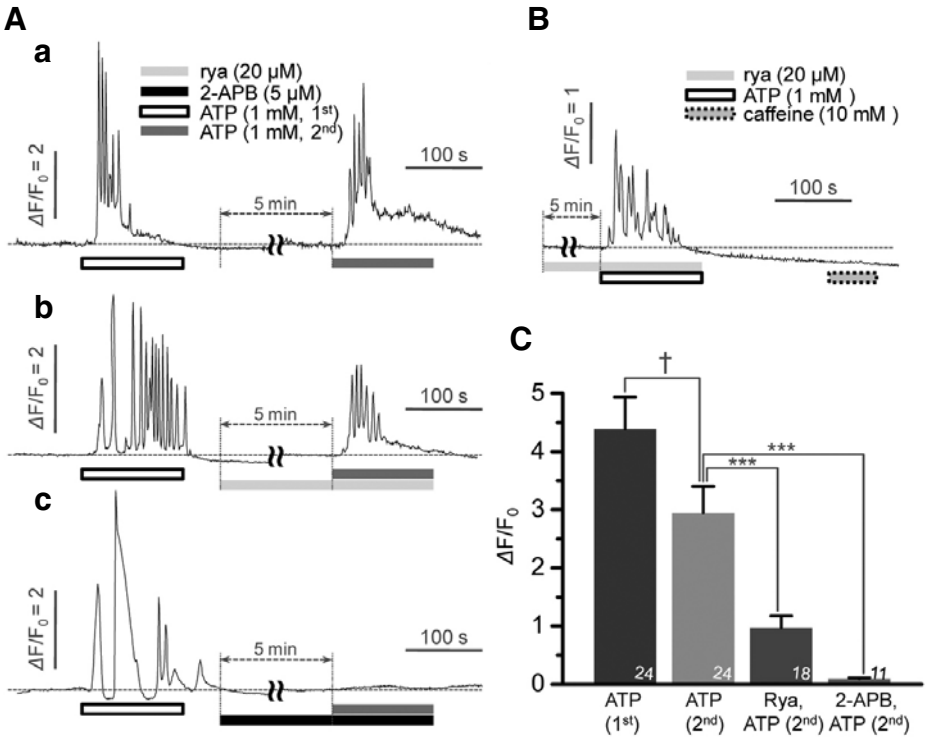

Fig. 4. Extracellular ATP-induced Ca^{2+} oscillation in HL-1 cells: roles of IP_3R and RyR. (A) Time courses of Ca^{2+} fluorescence ratio (2.38 Hz) measured from whole cell under the repeated applications of 1 mM ATP. Before the second application of ATP, some of the cells were pre-treated with 20 μM ryanodine (b) or 5 μM 2-APB (c) for 5 min. (B) Time course of Ca^{2+} change in an HL-1 cell, pre-incubated with 20 μM ryanodine for 5 min, under the application of 1 mM ATP and 10 mM caffeine. Bars under the Ca^{2+} traces indicate the period of each intervention. (C) Comparison of mean levels of ATP-induced Ca^{2+} increases in HL-1 cells during the first ("ATP (1^{st})") and second ("ATP (2^{nd})") exposure to ATP (n = 24) and comparisons of mean values of Ca^{2+} increases during the second exposure to ATP in cells that were pre-treated with control solution ("ATP (2^{nd})", n = 24), 20 μM ryanodine (rya, n = 18) and 5 μM 2-APB (2-APB, n = 11).

caine, which is known to reduce the open probability of the RyR channel by 98% in permeabilized cardiac cells (Bare et al., 2005), for ≥ 5 min.

Exposure to IP_3 (5, 10, 20, and 40 μM) elicited increases of the Ca^{2+} signal in the cytosol and nucleus in a concentration-dependent manner (Figs. 5A-5C). There was no significant difference in the peak magnitudes of cytosolic and nuclear Ca^{2+} changes for the different concentrations of IP_3 (Fig. 5A and 5C). Relatively high concentrations of IP_3 (20 and 40 μM) produced global Ca^{2+} oscillations (Figs. 5A and 5B). The frequency of Ca^{2+} oscillation was dependent on the IP_3 concentration (Fig. 5D, left graph). Mean frequency of IP_3-induced Ca^{2+} oscillations was 0.21 ± 0.03 events/s at 20 μM IP_3 (n = 6) and 0.32 ± 0.03 events/s at 40 μM IP_3 (n = 16). The Ca^{2+} oscillation lasted significantly longer at 40 μM IP_3 than at 20 μM IP_3, and the number of Ca^{2+} spikes during the Ca^{2+} oscillation was dependent on the IP_3 concentration (Fig. 5D, right graph; P < 0.05, 20 *vs.* 40 μM IP_3).

The IP_3 (40 μM)-induced Ca^{2+} increases in permeabilized HL-1 cells were almost completely inhibited by the pre-exposure to the IP_3R blockers, 2-APB (5 μM) or heparin (0.5 mg/ml) (Figs. 6B and 6D; control [in $\Delta F/F_0$]: cytosol, 0.93 ± 0.16, nucleus, 0.97 ± 0.18, n = 37; heparin: cytosol, 0.12 ± 0.02, nucleus, 0.10 ± 0.01, n = 25, P < 0.0001 *vs.* control; 2-APB: cytosol, 0.04 ± 0.01, nucleus, 0.07 ± 0.01, n = 29, P < 0.0001 *vs.* control), suggesting that the IP_3-dependent local Ca^{2+} signals are mediated by IP_3Rs.

Spatio-temporal properties of local Ca^{2+} signals induced by IP_3

Interestingly, the IP_3-induced local Ca^{2+} increases had at least two different phases, one with a slow monophasic rise and decay (*dashed trace* in Fig. 7A), and another with more rapid Ca^{2+} oscillations, the two phases were dissected as shown in the Fig. 7A ("**mon**ophasic Ca^{2+} transient" and "**osc**illatory change"). Interestingly, we found that the mean peak value (P_{mon}) of the slow monophasic Ca^{2+} changes was significantly higher in the nucleus than in the cytosol (Figs. 5A, 5B, and 7B). In sharp contrast, the magnitudes (P_{osc}) of the Ca^{2+} spikes during the Ca^{2+} oscillation were significantly larger in the cytosol than in the nucleus (Figs. 5A, 5B, and 7C). Such properties became clear when the Ca^{2+} oscillation was highly developed at 40 μM IP_3. These results suggest that Ca^{2+} oscillation during IP_3 exposure may be originated from cytosolic Ca^{2+} store and that the source of the slow monophasic Ca^{2+} transient may be the nucleus.

After exposure to IP_3 (40 μM), a Ca^{2+} increase was initiated from one side of the nucleus in a cell ("*Cell i*", *arrow in* Fig. 8Aa; "1" in Fig. 8B). In "*Cell i*", nuclear Ca^{2+} signals ("1" and "2") induced by IP_3, appeared to be monophasic, while an increase in the cytosolic Ca^{2+} accompanied a robust Ca^{2+} oscillation with a delay ("3", Figs. 8Ag and 8B). Ca^{2+} oscillation was also more pronounced in the cytosol of "*Cell ii*" ("6", Fig. 8B). In "*Cell ii*", the Ca^{2+} oscillation first occurred from the cytosol with a slight increase in the basal Ca^{2+} level ("6", Fig. 8B). Nuclear Ca^{2+} signals in "*Cell ii*" exhibited some Ca^{2+} oscillation, but its level was lower than that in the cytosol ("5", Fig. 8B). These results further support the idea that IP_3-dependent Ca^{2+} oscillation originates from the cytosol, and that IP_3 produces non-oscillating monophasic Ca^{2+} transient in the nucleus.

DISCUSSION

In the present study, we show significant expressions of IP_3R1 and IP_3R2, the peri-nuclear distribution of IP_3R1, and the cytoplasmic localization of IP_3R2 in HL-1 cells. Using confocal Ca^{2+} imaging in intact and permeabilized HL-1 cells, we demonstrated that IP_3Rs mediate transient intracellular Ca^{2+} increases in HL-1 cells. The assessment of the time courses of Ca^{2+} signals in the cytosol and nucleus enabled us to distinguish between two components in IP_3-induced Ca^{2+} increases: Ca^{2+} oscillation and the monophasic Ca^{2+} transient. The Ca^{2+} oscillation was robust and

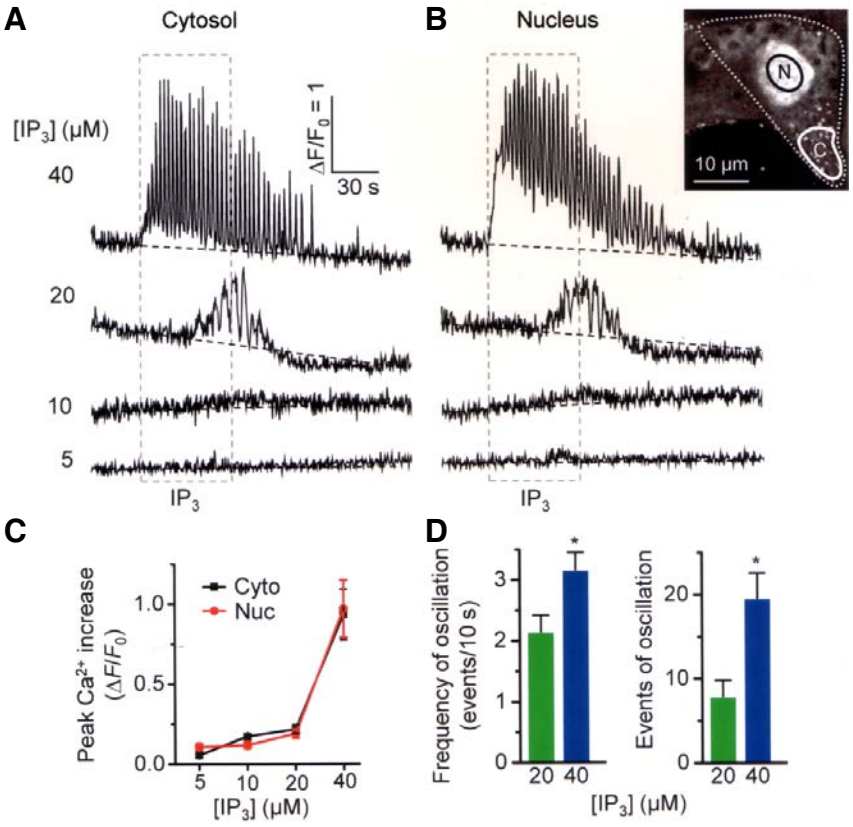

Fig. 5. IP_3-induced local Ca^{2+} changes in permeabilized HL-1 cells. Time courses of changes of local Ca^{2+} fluorescence (F/F_0) signals (2.38 Hz) measured from local area in the cytosol (A) and the nucleus (B) at different concentrations of IP_3 (40, 20, 10, and 5 μM). Inset image besides the panel B represents the confocal image of syto-11 fluorescence including ROIs ("N": nucleus; "C": cytosol) in HL-1 cell. The dashed box in the traces indicates the period of IP_3 exposure. (C) Mean levels of IP_3-induced local Ca^{2+} increases in the cytosol ("Cyto") and the nucleus ("Nuc"). (D) Mean frequency of the Ca^{2+} oscillations (left) and mean number of Ca^{2+} spikes during Ca^{2+} oscillation (right) at 20 (n = 6) and 40 μM (n = 16) IP_3.

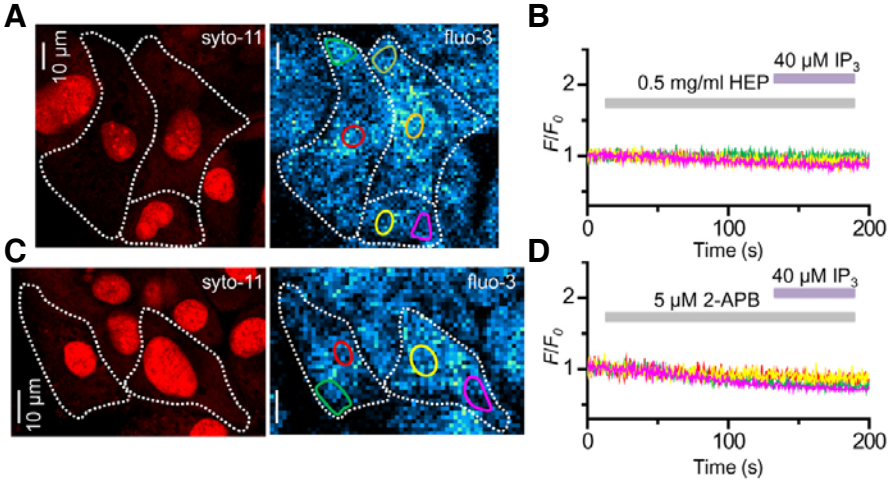

Fig. 6. Blockade of IP_3-induced Ca^{2+} releases by the blockers of IP_3R, heparin (HEP) and 2-APB. (A) and (C) show confocal images of HL-1 cells stained with syto-11, a nucleus dye (left), and Ca^{2+} images with regions-of-interest (ROI, right) where the F/F_0 traces in (B) and (D) were measured, respectively. The F/F_0 traces (2.38 Hz) in (B) and (D) show local Ca^{2+} signals measured from the indicated ROIs. Cells were pre-in-cubated with 1 mM tetracaine, the blocker of RyRs.

greater in the cytosol than in the nucleus, whereas the monophasic Ca^{2+} transient was larger and clearer in the nucleus. These results suggest that the distinct properties of IP_3-induced local Ca^{2+} signals in the cytosol and nucleus may be mediated by two different subtypes of IP_3R (type 2 and type 1) specifically localized to the cytosol and nucleus.

Although the expression of IP_3Rs in HL-1 cells has not been reported, our results demonstrating the molecular expression of type 2 IP_3Rs in atrial and ventricular myocytes and the higher expression of this protein in atrial cells compared with ventricular cells (Fig. 2) are in a good agreement with those reported previously (Bare et al., 2005; Lipp et al., 2000). In addition to the IP_3R2, we found a significant expression of IP_3R1 both in the isolated atrial myocytes and HL-1 cells with higher density in HL-1 cells (Fig. 2). The molecular expression of IP_3R1 in atrial tissue has been previously reported (Lencesova et al., 2002). The higher expression of IP_3R1 in HL-1 cells compared with isolated atrial myocytes (Fig. 2A) and the localization of IP_3R1 to the nuclear envelope in HL-1 cells (Fig. 3) suggest that IP_3R1 has a significant role in the nucleus (*e.g.*, gene transcription) of cell line system compared to non-proliferating adult atrial myocytes. It should be also noted that, although IP_3R2 proteins are localized to peripheral junctional SR (Lipp et al., 2000), the subcellular distribution of IP_3R1 in isolated adult atrial cells has not been demonstrated. The negligible expression of IP_3R1 in ventricular cells (Fig. 2), and the nuclear and t-tubular

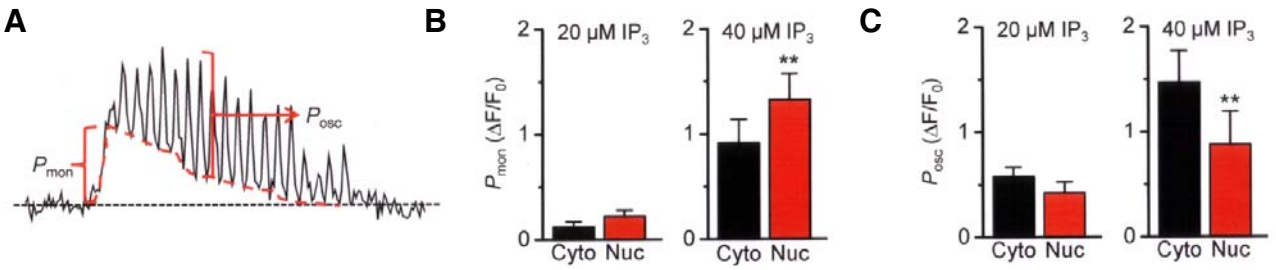

Fig. 7. Distinct spatio-temporal properties of IP_3-induced cytosolic and nuclear Ca^{2+}signals in HL-1 cells. (A) shows how the peak magnitudes of oscillations (P_{osc}) and monophasic Ca^{2+} rises (P_{mon}) were estimated from the IP_3-induced cytosolic and nuclear Ca^{2+} changes. (B) Comparisons of monophasic Ca^{2+} rises in the cytosol ("Cyto") and nucleus ("Nuc") when the cells were exposed to 20 (n = 6) and 40 μM (n = 16) IP_3. (C) Comparisons of mean magnitudes of Ca^{2+} oscillations in the cytosol and nucleus at 20 and 40 μM IP_3.

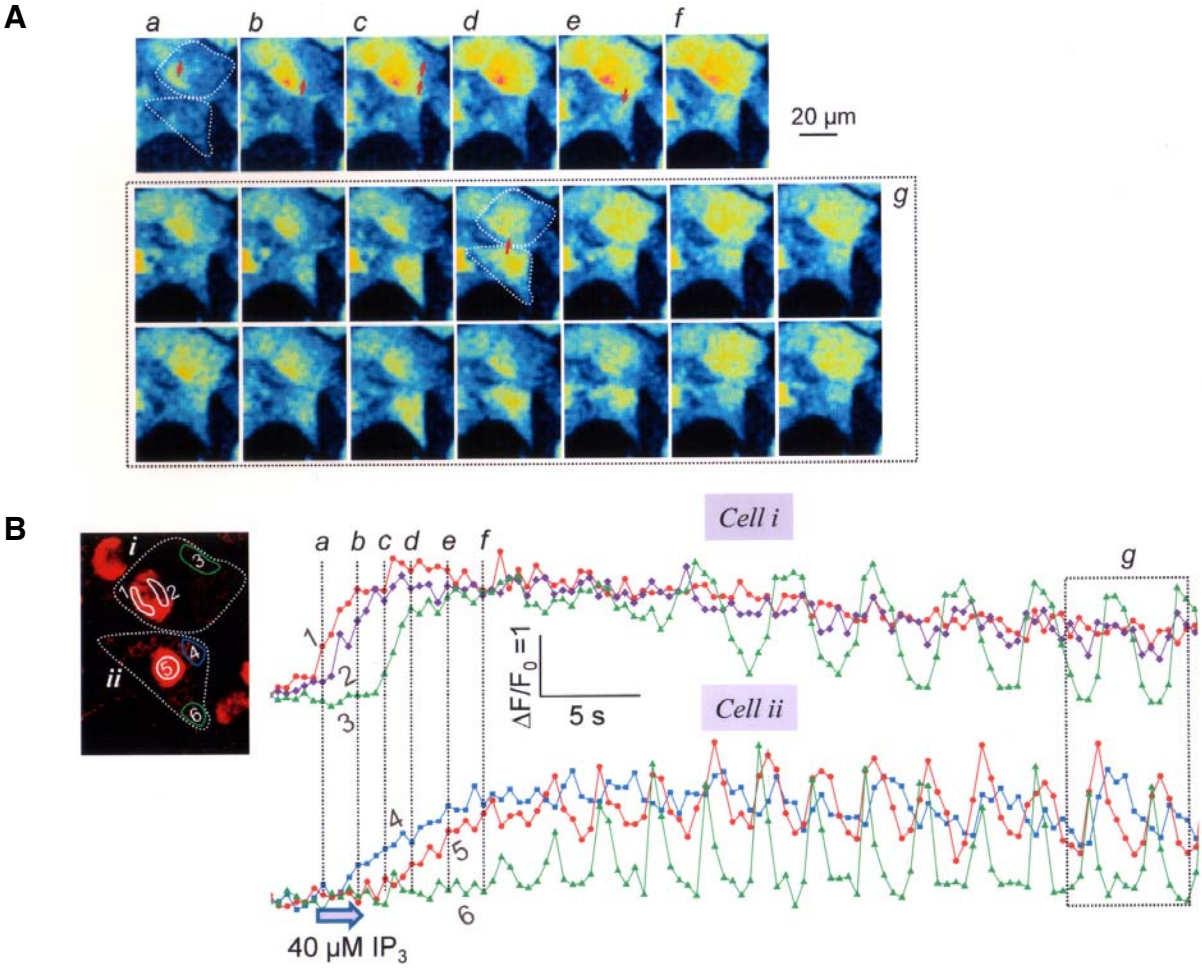

Fig. 8. Initiation and propagation of local Ca^{2+} signal on IP_3 exposure. (A) Confocal Ca^{2+} images measured in HL-1 cells (2.38 Hz) exposed to 40 μM IP_3. 2-D Ca^{2+} images were acquired at 2.38 Hz. The images were selected at the times indicated by the corresponding letters, *a~g,* in (B). (B) Left image shows confocal syto-11 image (: nucleus) in the same area, and map of ROIs ("1-6") which were used to measure the F/F_0 traces in (B), and position of cell *i* and cell *ii* (*dashed* line).

distribution of IP_3R2 at much lower levels in these cells (Bare et al., 2005; Mohler et al., 2005), may suggest that the IP_3R subtypes have distinct roles in ventricular and atrial myocytes. We were, however, unable to compare the expression levels of IP_3R2 with that of IP_3R1, perhaps because the IP_3R2 antibodies have a different quality in comparison with the IP_3R1 antibodies.

Exposure to ATP (1 mM) in the absence of external Ca^{2+} produced oscillatory Ca^{2+} releases via IP_3Rs in resting HL-1 cells (Fig. 4), which was somewhat similar to the local IP_3 responses observed in permeabilized HL-1 cells. The present data on ATP-mediated Ca^{2+} responses in HL-1 cells may also provide functional evidence for the expression of purinergic receptors in these cells, and support the proposition that HL-1 cells may be useful for studying the cardiac effects of purinergic

signaling.

To what extent biochemical and biophysical differences among IP_3R subtypes contribute to the regulation of global and local Ca^{2+} signaling in cardiac cells is not known. Based on the present results for HL-1 cells, there is distinct nuclear and cytosolic Ca^{2+} signaling under the stimulation of IP_3Rs, which may be related to the different contents of IP_3R subtypes in the nucleus and cytoplasm (Fig. 3). Distribution of the IP_3R2 as punctate forms, compared with the diffuse localization of the IP_3R1 (Fig. 3), indicates that the IP_3R2 may form clusters at specific spots in the SR domains. This is supported by a previous report on the formation of IP_3R2 clusters in resting conditions (Iwai et al., 2005). In fact, such clustering was demonstrated to be very important for the generation of Ca^{2+} oscillations by mathematical modeling (Shuai and Jung, 2003). The present observations related to the propensity for Ca^{2+} oscillation in the cytosol may be explained in part by the clustering of IP_3R2 in HL-1 cells.

Although there is a major subtype of IP_3R that mediates Ca^{2+} oscillation in a specific cell type, it appears that Ca^{2+} oscillation cannot be explained by a common functional result for a certain IP_3R subtype in various types of cells. Hattori et al. (2004) reported in HeLa cells and COS-7 cells, using measurements of whole-cell Ca^{2+} signal and siRNA methods, that IP_3R1 mediates Ca^{2+} oscillation and total Ca^{2+} signals, whereas IP_3R3 functions as an anti-Ca^{2+}-oscillatory unit. However, DT40 B cells expressing only IP_3R2 showed the most regular and robust Ca^{2+} oscillations, so that the cells expressing only IP_3R1 or IP_3R3 showed monophasic Ca^{2+} transient or rapidly damped Ca^{2+} oscillation only (Miyakawa et al., 1999).

When there was no bulk Ca^{2+} signal in the cytosol, the IP_3-induced nuclear Ca^{2+} increase did not have an oscillating component (Fig. 8B, trace "1"). The first Ca^{2+} release site during IP_3 exposure was often found to be in the nucleus. Considering the previous reports from reconstitution studies that IP_3R2 shows higher affinity for IP_3 than IP_3R1 while the affinity of IP_3R3 for IP_3 is lower, such a result was unexpected (Mikoshiba, 2007). Although it is not clear whether other nuclear components that can alter the activity of IP_3R1 are involved, the higher affinity of the nuclear Ca^{2+} signal to endothelin/IP_3 signaling has been reported in intact atrial cells (Kockskämper et al., 2008). Nuclear Ca^{2+} waves appeared to diffuse to the cytosol and trigger Ca^{2+} oscillation in the same HL-1 cell. IP_3-dependent nuclear Ca^{2+} waves have also been found in neonatal cultured ventricular myocytes (Luo et al., 2008).

The frequency of periodic increases in intracellular Ca^{2+} concentrations has been shown to be important for the efficiency and specificity of gene expression (Dolmetsch et al., 1998) and protein kinase activation (De Koninck and Schulman, 1998). Although specific functions of IP_3R subtypes in subcellular regions in atrial myocytes are not understood, one may expect in HL-1 cells that a IP_3-mediated long-lasting IP_3R-mediated Ca^{2+} signal in the nucleus may be more important for gene expressions, and that the IP_3-dependent Ca^{2+} oscillations may regulate the contractile function and membrane conductance. The specific impacts of Ca^{2+} releases via the IP_3R subtypes on the cardiac local Ca^{2+} signaling and gene regulation need further investigation. The present molecular and functional data on the expression of IP_3R subtypes in the HL-1 atrial cell line may provide a basis for using this cell line to study IP_3/IP_3R-mediated local Ca^{2+} signaling with genetic manipulations at the cellular levels.

ACKNOWLEDGMENTS

We thank Dr. W. Claycomb for HL-1 cells. This work was supported by National Research Foundation of Korea grants funded by the Ministry of Education, Science and Technology (2009-0053266, 2009-0065568, and 2009-0093815).

REFERENCES

Bare, D.J., Kettlun, C.S., Liang, M., Bers, D.M., and Mignery, G.A. (2005). Cardiac type 2 inositol 1,4,5-trisphosphate receptor. Interaction and modulation by calcium/calmodulin-dependent protein kinase II. J. Biol. Chem. *280*, 15912-15920.

Berridge, M.J. (2005). Unlocking the secrets of cell signaling. Annu. Rev. Physiol. *67*, 1-21.

Bootman, M.D., Collins, T.J., Mackenzie, L., Roderick, H.L., Berridge, M.J., and Peppiatt, C.M. (2002). 2-aminoethoxydiphenyl borate (2-APB) is a reliable blocker of store-operated Ca^{2+} entry but an inconsistent inhibitor of InsP3-induced Ca^{2+} release. FASEB J. *16*, 1145-1150.

Claycomb, W.C., Lanson, N.A. Jr., Stallworth, B.S., Egeland, D.B., Delcarpio, J.B., Bahinski, A., and Izzo, N.J. Jr. (1998). HL-1 cells: A cardiac muscle cell line that contracts and retains phenotypic characteristics of the adult cardiomyocyte. Proc. Natl. Acad. Sci. USA *95*, 2979-2984.

Danziger, R.S., Raffaeli, S., Moreno-Sanchez, R., Sakai, M., Capogrossi, M.C., Spurgeon, H.A., Hansford, R.G., and Lakatta, E.G. (1988). Extracellular ATP has a potent effect to enhance cytosolic calcium and contractility in single ventricular myocytes. Cell Calcium *9*, 193-199.

De Koninck, P., and Schulman, H. (1998). Sensitivity of CaM kinase II to the frequency of Ca^{2+} oscillations. Science *279*, 227-230.

Dolmetsch, R.E., Xu, K., and Lewis, R.S. (1998). Calcium oscillations increase the efficiency and specificity of gene expression. Nature *392*, 933-936.

Flores, R.V., Hernandez-Perez, M.G., Aquino, E., Gerrad, R.C., Weisman, G.A., and Gonzalez, F.A. (2005). Agonist-induced phosphorylation and desensitization of the $P2Y_2$ nucleotide receptor. Mol. Cell. Biochem. *280*, 35-45.

Furukawa, K., Pante, N., Aebi, U., and Gerace, L. (1995). Cloning of a cDNA for lamina-associated polypeptide 2 (LAP2) and identification of regions that specify targeting to the nuclear envelope. EMBO J. *14*, 1626-1636.

Hattori, M., Suzuki, A.Z., Higo, T., Miyauchi, H., Michikawa, T., Nakamura, T., Inoue, T., and Mikoshiba, K. (2004). Distinct roles of inositol 1,4,5-trisphosphate receptor types 1 and 3 in Ca^{2+} signaling. J. Biol. Chem. *279*, 11967-11975.

Hong, C.S., Cho, M.C., Kwak, Y.G., Song, C.H., Lee, Y.H., Lim, J.S., Kwon, Y.K., Chae, S.W., and Kim, D.H. (2002). Cardiac remodeling and atrial fibrillation in transgenic mice overexpressing junctin. FASEB J. *16*, 1310-1312.

Iwai, M., Tateishi, Y., Hattori, M., Mizutani, A., Nakamura, T., Futatsugi, A., Inoue, T., Furuichi, T., Michikawa, T., and Mikoshiba, K. (2005). Molecular cloning of mouse type-2 and type-3 inositol 1,4,5-trisphosphate receptors and identification of a novel type-2 receptor splice variant. J. Biol. Chem. *280*, 10305-10317.

Jaconi, M., Bony, C., Richards, S.M., Terzic, A., Amaudeau, S., Vassort, G., and Pucéat, M. (2002). Inositol 1,4,5-trisphosphate directs Ca^{2+} flow between mitochondria and the endoplasmic/sarcoplasmic reticulum: a role in regulating cardiac autonomic Ca^{2+} spiking. Mol. Biol. Cell *11*, 1845-1858.

Kim, J.C., Li, Y., Lee, S., Yi, Y.J., Park, C.S., and Woo, S.H. (2008). Effects of cryopreservation on Ca^{2+} signals induced by membrane depolarization, caffeine, thapsigargin and progesterone in boar spermatozoa. Mol. Cells *26*, 558-565.

Kitta, K., Clément, S.A., Remeika, J., Blumberg, J.B., and Suzuki, Y.J. (2001). Endothelin-1 induces phosphorylation of GATA-4 transcription factor in the HL-1 atrial-muscle cell line. Biochem. J. *359*, 375-380.

Kockskämper, J., Seidlmayer, L., Walther, S., Hellenkamp, K., Maier, L.S., and Pieske, B. (2008). Endothelin-1 enhances nuclear Ca^{2+} transients in atrial myocytes through $Ins(1,4,5)P_3$-dependent Ca^{2+} release from perinuclear Ca^{2+} stores. J. Cell Sci. *121*,186-195.

Lee, S., Kim, J.C., Li, Y., Son, M.J., and Woo, S.H. (2008). Fluid pressure modulates L-type Ca^{2+} channel via enhancement of Ca^{2+}-induced Ca^{2+} release in rat ventricular myocytes. Am. J. Physiol. Cell Physiol. *294*, C966-C976.

Lencesova, L., Ondrias, K., Micutkova, L., Filipenko, M., Kvetnansky, R., and Krizanova, O. (2002). Immobilization stress elevates IP_3 receptor mRNA in adult rat hearts in a glucocorticoid-dependent

manner. FEBS Lett. *531*, 432-436.
Lin, W.W., and Chuang, D.M. (1993). Agonist-induced desensitization of ATP receptor-mediated phosphoinositide turnover in C6 glioma cells: comparison with the negative-feedback regulation by protein kinase C. Neurochem. Int. *23*, 53-60.
Lipp, P., Laine, M., Tovey, S.C., Burrell, K.M., Berridge, M.J., Li, W., and Bootman, M.D. (2000). Functional $InsP_3$ receptors that may modulate excitation-contraction coupling in the heart. Curr. Biol. *10*, 939-942.
Lukyanenko, V., and Györke, S. (1999). Ca^{2+} sparks and Ca^{2+} waves in saponin-permeabilized rat ventricular myocytes. J. Physiol. *521*, 575-585.
Luo, D., Yang, D., Lan, X., Li, K., Chen, J., Zhang, Y., Xiao, R.P., Han, Q., and Cheng, H. (2008). Nuclear Ca^{2+} sparks and waves mediated by inositol 1,4,5-trisphosphate receptors in neonatal rat cardiomyocytes. Cell Calcium *43*, 165-174.
Mackenzie, L., Bootman, M.D., Laine, M., Berridge, M.J., Thuring, J., Holmes, A., Li, W.H., and Lipp, P. (2002). The role of inositol 1,4,5-trisphosphate receptors in Ca^{2+} signaling and the generation of arrhythmias in rat atrial myocytes. J. Physiol. *541*, 395-409.
McWhinney, C.D., Hansen, C., and Robishaw, J.D. (2000). Alpha-1 adrenergic signaling in a cardiac murine atrial myocytes (HL-1) cell line. Mol. Cell. Biochem. *214*, 111-119.
Mendes, C.C., Gomes, D.A., Thompson, M., Souto, N.C., Goes, T.S., Goes, A.M., Rodrigues, M.A., Gomez, M.V., Nathanson, M.H., and Leite, M.F. (2005). The type III inositol 1,4,5-trisphosphate receptor preferentially transmits apoptotic Ca^{2+} signals into mitochondria. J. Biol. Chem. *280*, 40892-40900.
Mikoshiba, K. (2007). IP_3 receptor/Ca^{2+} channel: from discovery to new signaling concepts. J. Neurochem. *102*, 1426-1446.
Miyakawa, T., Maeda, A., Yamazawa, T., Hirose, K., Kurosaki, T., and Iino, M. (1999). Encoding of Ca^{2+} signals by differential expression of IP_3 receptor subtypes. EMBO J. *18*, 1303-1308.
Mohler, P.J., Davis, J.Q., and Bennett, V. (2005). Ankyrin-B coordinates the Na/K ATPase, Na/Ca exchanger, and $InsP_3$ receptor in a cardiac T-tubule/SR microdomain. PloS Biol. *3*, 2158-2167.
Moschella, M.C., and Marks, A.R. (1993). Inositol 1,4,5-trisphosphate receptor expression in cardiac myocytes. J. Cell Biol. *120*, 1137-1146.
Perez, P.J., Ramos-Franco, J., Fill, M., and Mignery, G.A. (1997). Identification and functional reconstitution of the type 2 inositol 1,4,5-trisphosphate receptor from ventricular cardiac myocytes. J. Biol. Chem. *272*, 23961-23969.
Pucéat, M., and Vassort, G. (1996). Purinergic stimulation of rat cardiomyocytes induces tyrosine phosphorylation and membrane association of phospholipase Cγ: a major mechanism for $InsP_3$ generation. Biochem. J. *318*, 723-728.
Sartiani, L., Bochet, P., Cerbai, E., Mugelli, A., and Fischmeister, R. (2002). Functional expression of the hyperpolarization-activated non-selective cation current If in immortalized HL-1 cardiomyocytes. J. Physiol. *545*, 81-92.
Shuai, J.W., and Jung, P. (2003). Optimal ion channel clustering for intracellular calcium signaling. Proc. Natl. Acad. Sci. USA *100*, 506-510.
White, S.M., Constantin, P.E., and Claycomb, W.C. (2004). Cardiac physiology at the cellular level: use of cultured HL-1 cardiomyocytes for studies of cardiac muscle cell structure and function. Am. J. Physiol. Heart Circ. Physiol. *286*, H823-H8239.
Woodcock, E.A., and Matkovich, S.J. (2005). Ins(1,4,5)P_3 receptors and inositol phosphates in the heart evolutionary artefacts or active signal transducers? Pharmacol. Ther. *107*, 240-251.
Wu, X., Zhang, T., Bossuyt, J., Li, X., Mckinsey, T.A., Dedman, J.R., Olson, E.N., Chen, J., Brown, J.H., and Bers, D.M. (2006). Local $InsP_3$-dependent perinuclear Ca^{2+} signaling in cardiac mycoyte excitation-transcription coupling. J. Clin. Invest. *116*, 675-682.
Zima, A.V., and Blatter, L.A. (2004). Inositol 1,4,5-trisphosphate-dependent Ca^{2+} signaling in cat atrial excitation-contraction coupling and arrhythmias. J. Physiol. *555*, 607-615.